Study on optical characteristics of $Nd:YVO_4/YVO_4$ composite crystal laser

Tao Li (李 涛)[1], Zhuang Zhuo (卓 壮)[1,2], Xiaomin Li (李晓敏)[1], Hongzhi Yang (杨宏志)[3], and Yongqiang Zhang (张永强)[1]

[1]*College of Physics and Electronics, Shandong Normal University, Ji'nan 250014*

[2]*Shanda Luneng Information & Technology Co., Ltd., Shandong University, Ji'nan 250100*

[3]*College of Information Science and Engineering, Shandong University, Ji'nan 250100*

Received October 23, 2006

Thermal effect in crystals is the main obstacle blocking diode-pumped solid state laser to get high and stable output power. Diffusion bonding crystal has been demonstrated to be an effective method to relieve the thermal lensing theoretically based on the numerical heat analysis to the end-pumped anisotropic laser crystal. The temperature distributions in $Nd:YVO_4/YVO_4$ composite crystal and conventional crystal were analyzed and compared. The end-pumped $Nd:YVO_4/YVO_4$ composite crystal laser was designed and set up with z-cavity. The maximum output powers of 9.87 W at 1064 nm and 6.14 W at 532 nm were obtained at the incident pump power of 16.5 W. The highest optical-optical conversion efficiencies were up to 59.8% at 1064 nm and 37.2% at 532 nm respectively.

OCIS codes: 140.3480, 140.3380, 140.6810, 190.2620.

High power diode-pumped all-solid-state lasers have recently attracted much more interest for their unique merits, such as long lifetime, compact structure, high stability, and optical-optical conversion efficiency etc.[1−6]. However, thermal effect control is very critical in highly scaling the output power of diode-pumped solid-state lasers to a few watts up especially for end pumping configuration. Large thermal gradient arises from the heat deposition within a very small volume near the pumping facet of the laser crystal in longitudinally pumping system, which results in thermal lensing and the strongest aberrations at the pumping facet. Low temperature reservations of the pumping surface and the crystal body could be adopted to relieve thermal effects and improve laser performance[7]. This can be done by using diffusion bonding of the doped $Nd:YVO_4$ crystal and non-doped YVO_4 one[8−11], which serves as a heat sink for the pumping surface. In this paper, the impacts of non-doped crystal on doped crystal in end pumping configuration are analysed theoretically and verified experimentally.

The $Nd:YVO_4/YVO_4$ composite crystal used in experiment provided by Coretech Crystal Co., is shown in Fig. 1. The dimensions of the doped $Nd:YVO_4$ and non-doped YVO_4 crystals were $3 \times 3 \times 7$ (mm) and $3 \times 3 \times 2$ (mm), respectively. The $Nd:YVO_4$ and YVO_4 crystals were polished precisely before diffusion bonding of the $Nd:YVO_4$ and YVO_4 crystals together. The facet of the YVO_4 crystal was coated for anti-reflection (AR) at 808 nm and high-reflection (HR) at 1064 nm, and the other side of $Nd:YVO_4$ crystal was AR coated at 808 and 1064 nm.

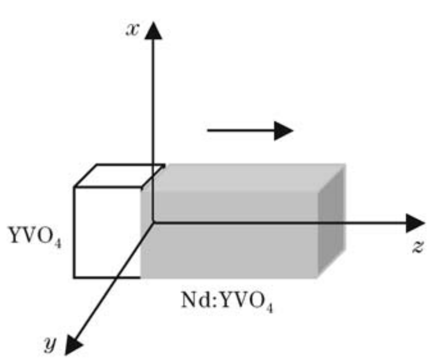

Fig. 1. $Nd:YVO_4/YVO_4$ composite crystal.

A schematic of the laser configuration is shown in Fig. 2. Both of $Nd:YVO_4/YVO_4$ and KTP crystals were water-cooled. The $Nd:YVO_4/YVO_4$ composite crystal was pumped by a fiber coupled diode laser at 808 nm. The radius of the pump beam was compressed to 0.32 mm on interface of the laser crystal. The $Nd:YVO_4/YVO_4$ composite crystal had a Nd^{3+} concentration of 0.5 at.-%. The pumping face of YVO_4 crystal served as one resonator mirror. The second-harmonic generator KTP crystal was $4 \times 4 \times 11$ (mm), and its facets were AR coated at 532 and 1064 nm.

A 4-mirror folded cavity was adopted in this experiment. Flat mirror M_1 coated on YVO_4 crystal acted as one resonator mirror, M_2 and M_3 were high reflective folded mirrors with radii of curvature of 20 and 10 cm, respectively. The output coupler M_4 was a flat mirror coated for HR at 1064 nm and AR at 532 nm.

Part of the absorbed pumping energy would be

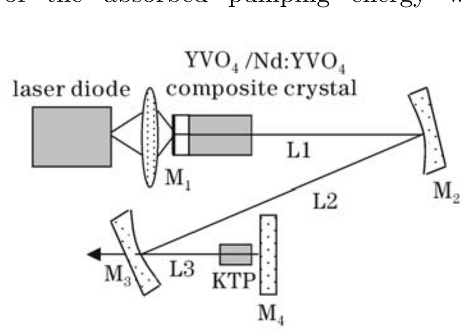

Fig. 2. Schematic of the $Nd:YVO_4/YVO_4$/KTP green light laser.

translated into heat dissipated in the laser crystal due to the quantum defect mechanism. The copper heat sink around the periphery of the composite crystal was water-cooled to keep at a constant temperature. Considering that the thermal conductivity of the heat sink is much greater than that of the crystal, the temperature at the surrounding facets of composite crystal was supposed to be a constant. The heat conduction in the crystal then can be analysed by the Possion equation as[12]

$$K_x \frac{\partial^2 T(x,y,z)}{\partial x^2} + K_y \frac{\partial^2 T(x,y,z)}{\partial y^2}$$
$$+ K_z \frac{\partial^2 T(x,y,z)}{\partial z^2} + q(x,y,z) = 0, \quad (1)$$

where $q(x,y,z)$ is the thermal density arising from the pumping power and K_x, K_y, K_z are the heat conductivities of the crystal at x, y, z orientations.

The thermal density $q(x,y,z)$ was assumed to be of Gaussian function along the resonator axis in the crystal[6],

$$q(x,y,z) = \frac{2Q\alpha}{\pi\omega_{\mathrm{p}}^2}(1-\mathrm{e}^{-\alpha l})\mathrm{e}^{-2[(x-\frac{a}{2})^2+(y-\frac{b}{2})^2]/\omega_{\mathrm{p}}^2}\mathrm{e}^{-\alpha z}, \quad (2)$$

where Q is the total thermal load, α the absorption coefficient, ω_{p} the Gaussian beam waist, l the crystal length, and a and b the side lengths of laser crystal.

Equation (1) can be solved numerically by Dirichlet method[13]. Supposing the heat sink temperature remained at $T_0 = 293$ K, both front and end facets of the composite crystal were heat insulated as they were directly exposed to air. The thermal distribution in the $Nd:YVO_4/YVO_4$ composite crystal was numerically calculated under the condition of 18-W pump power and 0.32-mm pump beam radius. The results were shown in Figs. 3 and 4.

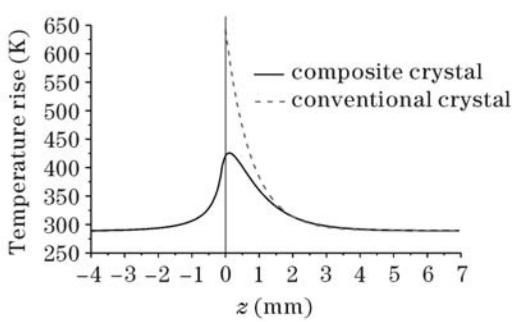

Fig. 3. Comparison of thermal distributions of the composite crystal with the conventional crystal.

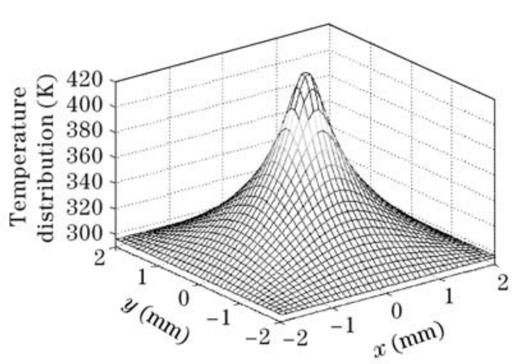

Fig. 4. Thermal distribution of $Nd:YVO_4/YVO_4$ composite crystal x-y section in $z = 0$.

The highest temperatures on the pumping surfaces of the $Nd:YVO_4/YVO_4$ composite crystal and $Nd:YVO_4$ crystal were 364 and 476 K, corresponding to the temperature rises of 71 and 183 °C, respectively. $Nd:YVO_4/YVO_4$ composite crystal was obviously an effective method to relieve the thermal dissipation.

The focal lengths of the $Nd:YVO_4/YVO_4$ composite crystal and $Nd:YVO_4$ crystal induced by thermal effect were obtained at different pump powers, as shown in Fig. 5.

The cavity parameters were rationally optimized on the above analysis. The lengths of three arms, L_1, L_2, and L_3, were 280, 200, and 110 mm, respectively. The total cavity length should be about 600 mm. Considering the thermal effects in laser crystal, the TEM_{00} mode radii inside the $Nd:YVO_4/YVO_4$ composite crystal and KTP can be calculated by

$$D = 2\sqrt{\frac{\lambda B}{\pi}}\left[1-\left(\frac{A+D}{2}\right)^2\right]^{-1/4}, \quad (3)$$

where λ is the oscillation wavelength.

Figure 6 shows the relationship between the available incident pump power and the TEM_{00} mode radii. As the pump power rising, the TEM_{00} mode diameter was remained at 600 μm, approximately equal to the pump beam waist of 640 μm.

The laser performance was investigated experimentally. The oscillation threshold was about 1.2 W, the maximum of 6.14-W continuous wave $Nd:YVO_4/YVO_4$/KTP green

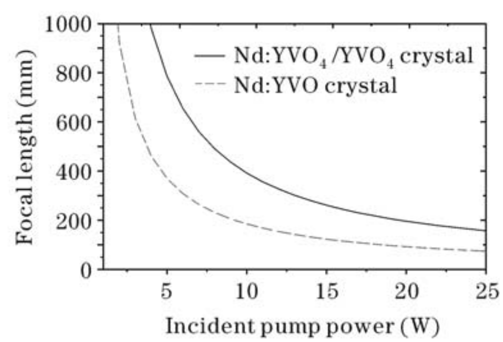

Fig. 5. Focal length versus pump power.

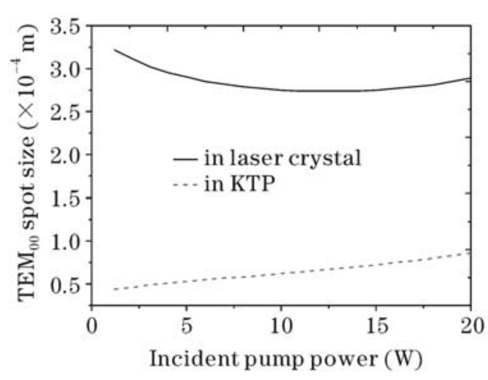

Fig. 6. Diameter of TEM_{00} spot of 1064 nm versus incident pump power.

Table 1. Output Power of Lasers at the Pump Power of 13 W

Time (min)	0	10	20	30	40	50	60	$\bar{P}$	$\Delta\bar{P}$
Output Power at 1064 nm (W)	7.50	7.50	7.51	7.50	7.51	7.50	7.51	7.504	0.013
Output Power at 532 nm (W)	5.03	5.14	4.81	5.13	5.04	5.11	5.27	5.076	0.096

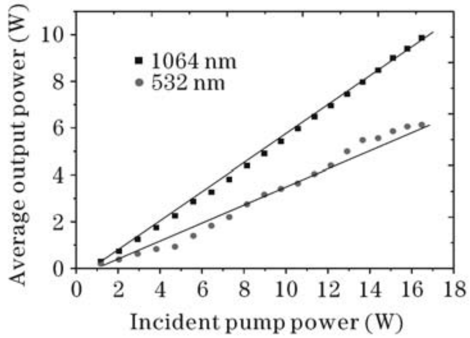

Fig. 7. Average output power at 1064 nm and 532 nm as a function of incident pump power.

laser was obtained at the incident pump power of 16.5 W, as shown in Fig. 7. The green laser operated at TEM_{00} mode while raising the LD pump power. The output power fluctuation $\Delta\bar{P}$ of the lasers was tested with LP-3C power meter at 1064 and 532 nm while the incident power operated at 15 W. The laser power was measured at a time interval of 10 minutes, as shown in Table 1. $\Delta\bar{P}$ was given by

$$\Delta\bar{P} = [\sum_{i-1}^{n}(P_i - \bar{P})^2/n]^{1/2}, \quad (4)$$

the stabilities $\Delta\bar{P}/\bar{P}$ of the laser at 1064 and 532 nm were 0.1% and 1.84% respectively.

In summary, thermal effect in laser diode end pumped laser was investigated numerically and experimentally in this paper. The heat depositions in Nd:YVO_4 crystal and Nd:YVO_4/YVO_4 composite crystals were analysed and compared, laser performances were tested to verify our results. A diode end pumped Nd:YVO_4/YVO_4 composite crystal green laser was designed by intracavity frequency doubling with KTP. The maximum output powers of 9.87 W at 1064 nm and 6.14 W at 532 nm were obtained at the pump power of 16.5 W. The highest optical-optical conversion efficiencies were 59.8% at 1064 nm and 37.2% at 532 nm, respectively.

This work was supported by the Science & Technology Research Fund of Shandong Province under Grant No. 031080125. The authors would like to appreciate for the support from Science & Technology Board of Shandong Province. Z. Zhuo is the author to whom the correspondence should be addressed, his e-mail address is z.zhuo@soullon.com.

References

1. J. Liu, Q. Peng, J. Yang, Q. Jiang, J. He, L. Qin, and X. Meng, Chin. Opt. Lett. **2,** 29 (2004).
2. M. E. Innocenzi, H. T. Yura, C. L. Fincher, and R. A. Fieids, Appl. Phys. Lett. **56,** 1831 (1990).
3. A. K. Cousins, IEEE J. Quantum Electron. **28,** 1057 (1992).
4. J. Liu, J. Yang, F. Liu, and J. He, Chin. Opt. Lett. **1,** 337 (2003).
5. H.-J. Moon, J. Yi, K.-S. Kim, B. Cha, and J. Lee, J. Korean Phys. Sov. **33,** 400 (1998).
6. C. Pfistner, R. Weber, H. P. Weber, S. Merazzi, and R. Gruber, IEEE J. Quantum Electron. **30,** 1605 (1994).
7. Z. Li, Z. Xiong, W. Huang, T. Chen, N. Moore, and G. C. Lim, Chin. J. Lasers (in Chinese) **32,** 297 (2005).
8. A. Sugiyama and Y. Nara, Ceram. Int. **31,** 1085 (2005).
9. M. Tsunekane, N. Taguchi, and H. Inaba, Appl. Opt. **37,** 5713 (1998).
10. R. H. Senn and L. E. Record, U.S. Patents US005394420A (1995).
11. A. Sugiyama, H. Fukuyama, T. Sasuga, T. Arisawa, and H. Takuma, Appl. Opt. **37,** 2407 (1998).
12. A.-M. Buoncristiani and C. E Byvik, IEEE J. Quantum Electron. **24,** 2253 (1988).
13. J. H. Mathews and K. D. Fink, *Numerical Methods Using MATLAB* (3rd end.) (House of Electronics Industry, Beijing, 2001) p.514.